Proceedings in Artificial Intelligence: Proceedings of the 3rd Workshop
"Dynamische Perzeption", Eds. G. Baratoff and H. Neumann,
PAI 9, pp. 135–140, Infix-Verlag, Berlin (2000)

Biologically Motivated Visual Control of Attitude and Altitude in Translatory Flight

Titus R. Neumann* and Heinrich H. Bülthoff

Max-Planck-Institut für biologische Kybernetik,
Spemannstraße 38, 72076 Tübingen

Abstract

Flying insects use highly efficient visual strategies for stabilizing their motion in three-dimensional space. We present a flight control model that uses a combination of biologically inspired, visual feed-forward mechanisms for stabilizing attitude (i.e. pitch and roll angles) and altitude during translatory motion. The attitude sensor exploits the position invariant vertical intensity gradient that exists in most natural open environments to orient the upper surface of a flying agent towards the region of maximum brightness (dorsal light response). Altitude is controlled using distance information contained in the frontoventral translatory optic flow (motion parallax). Our results from open-loop computer simulations show that the signals produced by these mechanisms robustly indicate the direction of deviation from a certain attitude angle or ground distance. We argue that in a closed control loop, these qualitative signals can be sufficient for flight stabilization. We present closed-loop trajectories of a simulated agent equipped with both mechanisms, flying over a textured, uneven surface. The agent shows robust flight behavior with six degrees of freedom.

1 Introduction

Biological studies over the last decades provided insight into many aspects of visual information processing and locomotion control in insects [3]. In spite of their extremely small brains, containing not more than a few million neurons, many insects show a remarkable performance in tasks like flight stabilization, obstacle avoidance, and navigation. It is assumed that the highly specialized, massive parallel information processing in the insect visual system contributes to the speed and robustness of these behaviors.

Previous studies of biologically motivated visual self-motion control and obstacle avoidance behavior in artificial systems are limited to motion in a horizontal or vertical plane with one or two degrees of freedom. Mura and Francheschini (1994) show a computer simulation of vertical obstacle avoidance and altitude control behavior, assuming pure forward motion in the vertical plane with fixed attitude angles [7]. Huber and Bülthoff (1997) demonstrate the simulated evolution of two-dimensional obstacle avoidance and tracking behavior in an artificial agent inspired by the visual system of the fly [5]. Srinivasan et al. (1999) apply several principles of insect vision such as rangefinding by “peering”, centering behavior, obstacle avoidance, and visual odometry to robot navigation on the ground plane [9].

However, motion in three-dimensional space has six degrees of freedom. In order to maintain a certain altitude when flying over a surface, they cannot be controlled independently from each other due to the anisotropy of the environment determined by gravity [4]. Body rotations about the yaw axis and altitude changes leave the lift force aligned with the direction of gravity, whereas deviations from neutral

*Corresponding author. mailto:titus.neumann@tuebingen.mpg.de

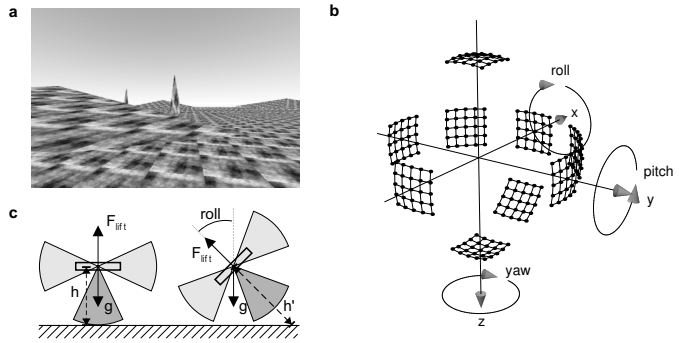

Figure 1: (a) Virtual environment with obstacles on a textured, uneven surface. (b) Light receptor directions (black dots) and body coordinate system of the agent. (c) Misalignment of body and world verticals causes erroneous altitude estimates and lateral drift.

attitude (i.e. roll and pitch angles not equal to zero) cause lateral motion and erroneous alitude estimates, as illustrated in Fig.1 c. Thus, flying over a surface in a gravity field requires attitude control.

In this study we present a biologically inspired model for visual stabilization of simulated 3D flight, including both attitude and altitude control. After a description of the model in the following section, simulation results are shown and discussed.

2 Simulation model

The flight control model is experimentally evaluated using a simulated agent flying through a three-dimensional virtual environment with a textured uneven surface (Fig.1 a). The visual input of the agent's light receptors is determined by ray casting. The distribution of the local viewing directions $\mathbf{d}_i$ of these receptors is shown in Fig.1 b. The agent is equipped with nine groups of 5x5 light receptors. For each receptor, nine samples of the intensity distribution around the receptor main axis are computed. The samples are averaged using Gaussian weighting with a half width of $4.0°$ at an inter-receptor angle of $6.0°$.

2.1 Attitude from intensity distribution

During daylight, most natural open environments exhibit an intensity gradient which is (a) perpendicular to the local average surface, (b) aligned with the direction of gravity, and (c) invariant with the observer's position on the surface. Many animals use this anisotropy of open environments to align their vertical body axis with the direction of gravity, particularly if they do not have direct contact to the surface. In flying insects and fish this mechanism is known as the dorsal light response, since these animals orient their back towards the region of maximum brightness in their visual environment.

Fig.2 a shows the working principle of the mechanism used in this simulation. The vertical intensity gradient of the environment is averaged separately by opposite hemispherical receptive fields. The response of each receptive field is maximal when the corresponding hemisphere is oriented towards the region of maximum brightness. Thus, the roll angle can be estimated as

$$\sigma_{\mathrm{aRoll}} = \sum_{\langle \mathbf{d}_i, \mathbf{e}_y \rangle \neq 0} \frac{\langle \mathbf{d}_i, \mathbf{e}_y \rangle}{|\langle \mathbf{d}_i, \mathbf{e}_y \rangle|} I_i, \tag{1}$$

where $\mathbf{e}_y = (0, 1, 0)$ is the y axis of the agent's body coordinate system, and I_i is the local intensity in viewing direction $\mathbf{d}_i$. The pitch angle estimate σ_{aPitch} is computed likewise, replacing $\mathbf{e}_y$ by $\mathbf{e}_x = (1, 0, 0)$.

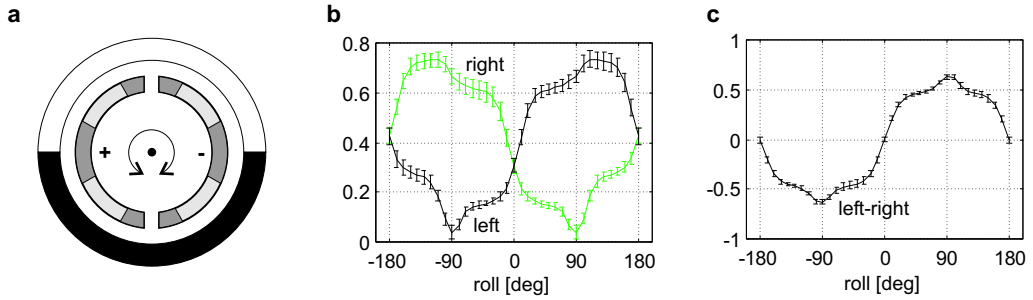

Figure 2: Visual attitude control by dorsal light response. (a) Model for attitude control. The vertical intensity gradient of the environment (outer ring) is averaged separately for the left and right hemispheres (inner ring, showing a vertical section through the receptor configuration in Fig.1 b). The difference of both signals reliably indicates the sign of the current roll angle. (b) Left and right average intensities as functions of roll angle, measured at 100 randomly selected positions and heading angles in the simulated environment. (c) Difference of left and right signals as a function of roll angle.

2.2 Distance information from translatory optic flow

In a stationary environment, for an observer translating with velocity $\mathbf{T}$ while rotating with velocity $\mathbf{R}$ about the origin of the body coordinate system the local optic flow in viewing direction $\mathbf{d}_i$ is

$$\mathbf{p}_i = -\frac{(\mathbf{T} - (\mathbf{T} \cdot \mathbf{d}_i)\,\mathbf{d}_i)}{D_i} - \mathbf{R} \times \mathbf{d}_i, \tag{2}$$

where D_i is the distance to the environment in the local viewing direction [6]. Assuming pure translatory motion with a constant velocity, the local optic flow is proportional to $1/D_i$.

In this simulation, for each viewing direction $\mathbf{d}_i$ the local optic flow Φ_i is estimated using elementary motion detectors (EMD) of the Reichardt correlation type, given by

$$\Phi(I_x, I_{x+\Delta x}) = L_{11}(H_1(I_x)) \cdot L_{22}(H_2(I_{x+\Delta x})) - L_{12}(H_1(I_x)) \cdot L_{21}(H_2(I_{x+\Delta x})). \tag{3}$$

I_x and $I_{x+\Delta x}$ are the intensity values measured by two neighbouring receptors. L_{11}, L_{12}, L_{21} and L_{22} are standard discrete time IIR temporal lowpass filters

$$L(I_t) = \left(1 - \frac{1}{\tau}\right) L(I_{t-1}) + \frac{1}{\tau} I_t \tag{4}$$

with time constants $\tau_{11} = \tau_{21} = 1.25$ and $\tau_{12} = \tau_{22} = 5.0$. H_1 and H_2 are temporal highpass filters

$$H(I_t) = I_t - L_H(I_t) \tag{5}$$

with time constant $\tau_H = 100.0$ for the corresponding lowpass L_H. Projecting the local flow vectors $\mathbf{p}_i$ expected for pure forward translation onto the EMD directions $\mathbf{u}_i$ yields a receptive field (matched filter) which responds maximally for translatory optic flow [2]. By using an appropriate window function $\delta(\mathbf{d}_i)$ the receptive field is restricted to the frontoventral region and has the form

$$\sigma_{\mathrm{vTxVentral}} = \sum_i \delta_i \Phi_i \left\langle \mathbf{p}_i, \mathbf{u}_i \right\rangle, \tag{6}$$

where Φ_i is the local image flow estimate.

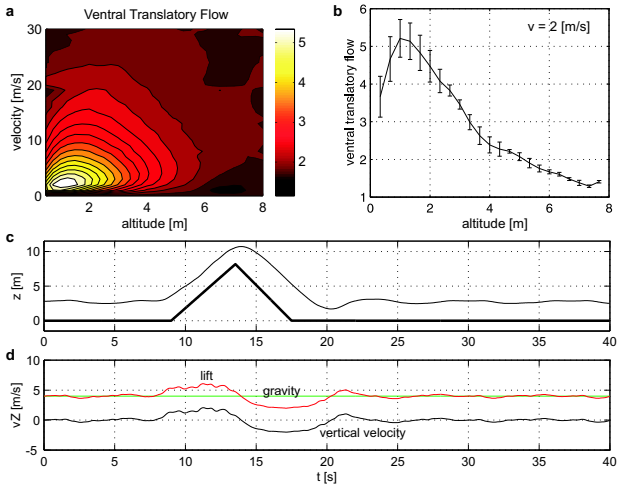

Figure 3: Visual altitude control in translatory flight. (a) Open-loop average frontoventral optic flow signal as a function of translatory velocity and altitude above surface. (b) Frontoventral motion signal at velocity $v_x = 2$ m/s. (c), (d) Time course of closed-loop altitude control. (c) Vertical component of flight trajectory (gray) and surface elevation (black). (d) Lift force (gray) proportional to the measured optic flow signal, and vertical velocity (black).

2.3 Control loop and flight dynamics

The motor system of the simulated agent is capable of generating roll, pitch and yaw torque as well as a lift force along the vertical body axis. The roll, pitch and lift motors are activated by the attitude and altitude sensors descibed above. In order to control yaw rotations, two additional visual sensors for course stabilization (optomotor response, OMR) and obstacle avoidance (OA) are included, estimating the rotational optic flow about the yaw axis (σ_{vYaw}) and the frontolateral left and right translational flow ($\sigma_{\mathrm{vTxLeft}}$ and $\sigma_{\mathrm{vTxRight}}$), respectively [3],[5]. For each simulation step, the motor activation vector

$$\mathbf{m} = (\mu_{\mathrm{roll}}, \mu_{\mathrm{pitch}}, \mu_{\mathrm{yaw}}, \mu_{\mathrm{lift}}) \tag{7}$$

is updated with the vector of current sensor signals

$$\mathbf{s} = (\sigma_{\mathrm{aRoll}}, \sigma_{\mathrm{aPitch}}, \sigma_{\mathrm{vYaw}}, \sigma_{\mathrm{vTxVentral}}, \sigma_{\mathrm{vTxLeft}}, \sigma_{\mathrm{vTxRight}}) \tag{8}$$

using the connection weight matrix $\mathbf{W}_{\mathrm{sm}}$:

$$\mathbf{m} = \mathbf{s}\mathbf{W}_{\mathrm{sm}} = \mathbf{s} \begin{pmatrix} -w_{\mathrm{roll}} & 0 & 0 & 0 \\ 0 & -w_{\mathrm{pitch}} & 0 & 0 \\ 0 & 0 & -w_{\mathrm{OMR}} & 0 \\ 0 & 0 & 0 & w_{\mathrm{lift}} \\ 0 & 0 & w_{\mathrm{OA}} & 0 \\ 0 & 0 & -w_{\mathrm{OA}} & 0 \end{pmatrix}. \tag{9}$$

The instantaneous velocity of the simulated agent is set proportional to the applied motor force, ignoring its mass and inertia. This approximation is valid for small flying insects such as *Drosophila*, since they experience strong drag from air viscosity [8], entirely compensating for the propulsion force after a short initial acceleration. Therefore, in this simulation the vertical velocity of the agent is chosen proportional to the difference of lift force and gravitational force.

3 Results and discussion

3.1 Attitude control

Visual attitude control is based on balancing the average intensities measured by opposite hemispherical receptive fields. Fig.2 b shows the signals of the left and right receptive fields as functions of the roll angle,

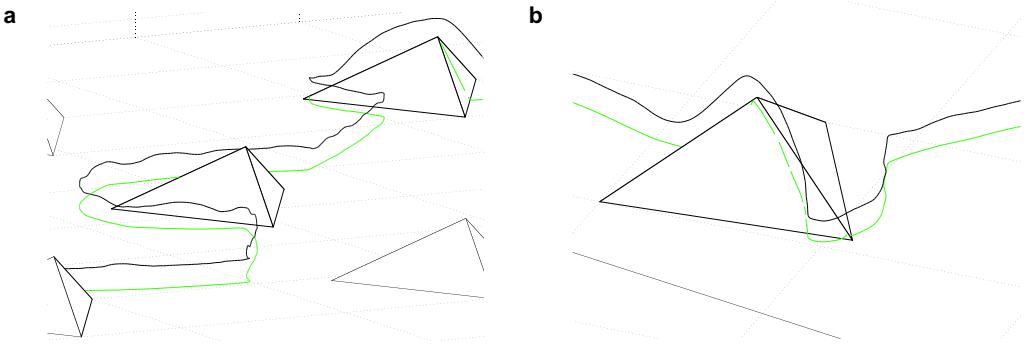

Figure 4: Closed-loop 3D flight behavior of a simulated agent equipped with attitude and altitude control in an open environment containing pyramid-shaped obstacles. (Trajectories: black; projection on the surface: gray. The surface texture is not shown.)

measured at 100 randomly selected positions and heading angles in the virtual environment. The response of each receptive field is maximal when the hemisphere is oriented towards the region of maximum brightness. The difference between the signals from two opposite hemispheres reliably indicates the sign of the current attitude angle (Fig.2 c).

The described visual attitude sensor uses a global intensity gradient that exists in open environments. Thus, it detects the average surface normal which needs to be approximately aligned with the direction of gravity in order to achieve successful self-motion stabilization. Additional mechanisms for attitude stabilization are required if the entire visible surface is slanted, if the agent is very close to a single large object, or if the intensity gradient does not exist or is even reversed, e.g. in closed rooms or over a reflecting snow or water surface.

3.2 Altitude control

For altitude control, the average translatory optic flow in the frontoventral visual field is used. Fig.3 a shows the flow signal as a function of translatory velocity and altitude above ground. The signal has a maximum at $v_x = 2$ m/s and decreases slowly with increasing velocity, showing a typical correlation-type EMD tuning curve. Since the signal also decreases with increasing altitude h for $h \geq 1$ m (Fig.3 b), it can be used to modulate the lift force in a closed control loop (Fig.3 c and d). Hence, the signal is sufficient for altitude control although the EMDs do not measure the true image velocity.

The described algorithm assumes translatory motion of the agent. Simultaneous rotations can corrupt the ventral translational flow, impairing the ground distance estimation. Additional mechanisms such as the optomotor response in flies [3] can be used to inhibit rotatory motion. If rotations are inevitable, e.g. for attitude correction or obstacle avoidance, the duration can be minimized by fast, saccadic turns. During these saccades the flow signal can be suppressed, or a rotational velocity beyond the sensitivity of the detectors for translatory motion can be chosen. Since translatory flow is required to yield distance information, this mechanism cannot be used for hovering.

3.3 Closed-loop flight behavior

Fig.4 shows closed-loop 3D trajectories of a simulated agent flying autonomously through a virtual open environment containing large pyramid-shaped obstacles. The agent maintains its altitude during obstacle avoidance maneuvers (a) and follows the terrain elevation (b).

3.4 Conclusion

The open-loop simulation results show that the signals from two simple biologically inspired visual detectors robustly indicate the direction of deviation from a neutral attitude or a certain ground distance. In closed-loop experiments, a simulated agent equipped with both mechanisms shows robust flight behavior with six degrees of freedom over a textured, uneven terrain. We conclude that (a) in a closed control loop, qualitative signals can be sufficient for flight stabilization, and (b) the control of complex behaviors such as 3D flight can be facilitated by functional decomposition into elementarty tasks, in this case into separate mechanisms for attitude and altitude control.

The presented mechanisms are purely reactive and do not require working memory. They are based on a massive parallel feed-forward connectivity with few sequential processing steps. The connection scheme is adapted to specific tasks under specific constraints and therefore does not change during computation, facilitating possible hardware implementations such as analog VLSI (very large scale integration). Simple robust control algorithms will be crucial for autonomous vehicle guidance and robotics, especially in applications with strong constraints in size, weight, and energy consumption, such as aerospace and nano-robotics.

Acknowledgments This work was supported by the Flughafen Frankfurt Main Stiftung and the Max Planck Gesellschaft.

References

[1] Egelhaaf, M., Borst, A. (1993). Movement detection in arthropods. In F.A. Miles & J. Wallman (Eds.), *Visual motion and its role in the stabilization of gaze*, pp. 53 - 77. Amsterdam: Elsevier.

[2] Franz, M.O., Neumann, T.R., Plagge, M., Mallot, H.A., Zell, A. (1999). Can fly tangential neurons be used to estimate self-motion? *Proceedings of the 9th international conference on artificial neural networ*ks *ICANN99*, pp. 994 - 999. Berlin: Springer Verlag.

[3] Götz, K.G. (1968). Flight control in *Drosophila* by visual perception of motion. *Kybernetik*, **4**(6), 199 - 208.

[4] Hengstenberg, R., Sandeman, D.C., Hengstenberg, B. (1986). Compensatory head roll in the blowfly *Calliphora* during flight. *Proc. R. Soc. Lond.*, B **227**, 455 - 482.

[5] Huber, S.A., Bülthoff, H.H. (1997). Modeling obstacle avoidance behavior of flies using an adaptive autonomous agent. *Proceedings of the 7th international conference on artificial neural networ*ks *ICANN97*, pp. 709 - 714. Berlin: Springer Verlag.

[6] Koenderink, J.J., van Doorn, A.J. (1987). Facts on optic flow. *Biol. Cybern.*, **56**, 247 - 254.

[7] Mura, F., Franceschini, N. (1994). Visual control of altitude and speed in a flying agent. In D. Cliff, P. Husbands, J.-A. Meyer, & S.W. Wilson (Eds.), *From Animals to Animats 3: Proceedings of the third international conference on simulation of adaptive behav*ior *SAB94*, pp. 91 - 99. Cambridge, MA: MIT Press/Bradford Books.

[8] Nachtigall, W. (1968). Insects in Flight. New York: McGraw-Hill.

[9] Srinivasan, M.V., Chahl, J.S., Weber, K., Venkatesh, S., Nagle, M.G., Zhang, S.W. (1999). Robot navigation inspired by principles of insect vision. *Robotics and Autonomous Systems*, **26**, 203 - 216.

[10] Srinivasan, M.V., Zhang, S.W., Chahl, J.S., Barth, E., Venkatesh, S. (2000). How honeybees make grazing landings on flat surfaces. *Biol. Cybern.*, **83**, 171 - 183.